Journal of Sustainable Metallurgy
https://doi.org/10.1007/s40831-025-01070-x

RESEARCH ARTICLE

Nanohydrometallurgy with Superparamagnetic Nanoparticles: A Sustainable Solution for Critical Metal Retrieval from Phosphogypsum

Giovani Pavoski[1,2] · Denise Crocce Romano Espinosa[1] · Jorge Alberto Soares Tenório[1] · Wenying Liu[2]

Received: 12 September 2024 / Accepted: 14 March 2025

Abstract

This study evaluates the efficiency and selectivity of nanohydrometallurgy for the recovery of critical metals from phosphogypsum leachates using functionalized superparamagnetic nanoparticles (Si@Fe-DTPA). The extraction process was tested in monometallic, multimetallic, and leachate synthetic solutions containing Ce, Dy, La, Nd, and Y. The results demonstrated that selective separation is achievable, with extraction efficiencies of 17.59% for Ce, 5.96% for Dy, 13.74% for La, 19.83% for Nd, and 12.93% for Y in a single cycle. The selectivity order for Si@Fe-DTPA was Nd > Y > La > Dy > Ce, confirming its preferential affinity for specific rare earth elements. The contaminant metal Ca, present in the highest concentration, was efficiently removed within three cycles. The overall process required 10 to 20 cycles to obtain high-purity fractions of critical metals. The findings confirm that nanohydrometallurgy is a sustainable and effective technique for critical metal recovery, offering an alternative to traditional extraction methods and contributing to the circular economy. This approach aligns with the United Nations Sustainable Development Goals (SDGs) by reducing dependence on primary mining sources and promoting resource efficiency.

Graphical Abstract

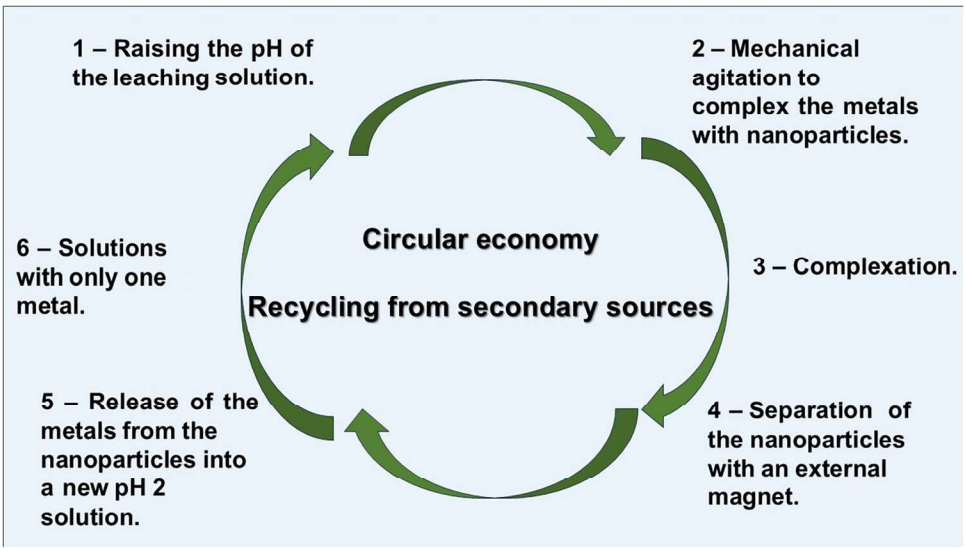

Keywords Nanohydrometallurgy · Circular economy · Superparamagnetic nanoparticles · Recycling · Rare earth metals

Abbreviations

COO^-	Carboxylate group
DTPA	Diethylenetriaminepentaacetic Acid
EAPTMS	Ethylenediaminepropyltrimethoxysilane

The contributing editor for this article was Anna Kaksonen.

Extended author information available on the last page of the article

Published online: 07 April 2025

Fe_3O_4	Magnetite
Hrees	Heavy rare earth elements
ICP-OES	Inductively Coupled Plasma Optical Emission Spectrometry
Lrees	Light rare earth elements
NH_2	Amine group
Nps	Nanoparticles
$RE(CO_3)_3^{3-}$	Rare Earth Carbonate Complex
Rees	Rare earth elements
Rems	Rare earth metals
SiO_2	Silicon Dioxide (Silica)
Si@Fe-DTPA	Superparamagnetic magnetite nanoparticles functionalized with DTPA
Snps	Superparamagnetic nanoparticles
TEOS	Tetraethyl Orthosilicate

Introduction

The advancement of technology and the synthesis of new materials have increased investments in the mining industry for the extraction of strategic metals from primary sources [1]. Similarly, investments in the recycling industry have grown for the recovery of these metals from secondary sources [2]. Consequently, all established hydrometallurgical techniques are being researched to identify the optimal methodologies for these processes.

Nanohydrometallurgy is an advanced technique that integrates nanotechnology with hydrometallurgical processes, offering an innovative approach to selective metal separation [3]. This method utilizes functionalized superparamagnetic nanoparticles (Snps) that selectively bind to metal ions through surface interactions, enabling efficient extraction from complex solutions. Unlike conventional separation methods, Snps can be rapidly recovered using an external magnetic field, allowing for their reuse in multiple cycles, minimizing reagent consumption, and reducing waste generation. Nanohydrometallurgy complements established techniques such as selective precipitation [4], organic solvent extraction [5], ion exchange resins [6], electrodeposition [7], and electrodialysis [8]. While these techniques differ in their mechanisms, they share a common goal: achieving highly selective and sustainable metal recovery [9].

Solvent extraction and ion exchange resins are the most widely used advanced techniques for recovering metals from primary and secondary sources, each with its own advantages and challenges. Nanohydrometallurgy is being developed as an alternative and complement. The use of Snps has already shown promise and efficiency [10], which complex with the metals of interest and can be easily separated from other metals through the application of a magnetic field. The high efficiency of this methodology stems from the use of nanoparticles (Nps), which have a large surface area and can be surface-functionalized with different complexing agents to enhance specificity for the target metal.

Snps are particularly advantageous because permanent magnets do not require electricity, simplifying operations such as filtration, concentration, and washing. Additionally, the magnetic confinement process allows the entire procedure to be conducted in a single reactor, at room temperature, with high recyclability [11–14]. Despite all these advantages, the separation of concentrated solutions has not yet been fully tested, and higher efficiency is still achieved with other techniques.

Solvent extraction is widely used due to its high efficiency in separating metals from aqueous solutions. The use of organic solvents allows for selective extraction and effective purification, which is essential for obtaining high-purity products [15–17]. However, the toxicity of the solvents and waste management pose significant environmental challenges. This technique is well-established in various industries, but its efficiency is counterbalanced by the need for frequent solvent replacement and associated costs. Ion exchange, on the other hand, utilizes specific resins to capture metal ions, offering an efficient and reusable solution [18–20]. Although it is a clean and sustainable technique, its application is limited by the capacity of the resins and the costs of regeneration. These technologies offer promising solutions for metal recovery, but each requires optimization to address the associated environmental and economic challenges.

Rare earth metals (Rems), including elements like the lanthanides and certain transition metals, are essential to modern technology due to their unique properties. These metals are critical for producing high-performance magnets, phosphors for lighting and displays, and catalysts in petroleum refining. While Rems are not relatively abundant in the Earth's crust, they are not typically found in concentrated deposits [21–23]. Rems are also included in the list of critical metals. These elements are essential to the modern economy due to their application in a wide range of technological and industrial sectors, yet they face a significant risk of supply shortage. In the European Union, the list of critical metals is defined based on two main parameters: economic importance and supply risk. Key minerals rich in rare earth elements include bastnäsite, primarily composed of light Rees such as Ce (45–50%), La (20–25%), and Nd (10–15%); monazite, containing Ce (30–50%), La (15–30%), Nd (10–25%), and up to 12% Th; and xenotime, a major source of heavy Rees, with Y (50–60%), Dy (3–10%), and other Hrees in lower concentrations [24–26].

Beyond primary sources, Rems are also found in various industrial by-products. Phosphogypsum, a by-product of phosphate fertilizer production, contains rare earth elements at concentrations ranging from 400 to 1000 mg/kg or approximately 0.05 wt% to 1.5 wt% of rare earth oxides (REOs),

depending on the ore and production process [27]. Bauxite residue (red mud), a by-product of alumina extraction, has drawn attention due to its large-scale generation (120–150 million tons per year) and the presence of Rees (0.5–1.7 kg per ton), particularly scandium (Sc), with reported Rem concentrations between 100 and 2000 mg/kg [28]. Coal fly ash, a by-product of coal combustion in power plants, has been recognized as a potential secondary source of Rees. Its Rem content typically ranges from 200 to 500 mg/kg, depending on coal type and combustion conditions. A study analyzing 581 ash samples from power stations across 15 countries reported an average Ree concentration of 435 mg/kg, slightly higher than the 404 mg/kg previously documented [29, 30]. Spent catalysts from petroleum refining, which are widely used in chemical processes, can also contain valuable Rems. In particular, they may have lanthanum (La) concentrations ranging from 2 to 5 wt%, depending on catalyst composition and usage conditions [31].

Phosphogypsum, composed primarily of gypsum (calcium sulfate, $CaSO_4$), can also contain trace amounts of rare earth elements, including lanthanides such as cerium (Ce), dysprosium (Dy), neodymium (Nd), and yttrium (Y). The presence of these Rems in phosphogypsum highlights its potential as a secondary source of valuable materials [32–34]. The recovery of Rems from phosphogypsum is essential to meet growing demand in high-tech sectors, such as electronics, renewable energy, and advanced manufacturing. Hydrometallurgical techniques are commonly employed to extract these metals from phosphogypsum [27, 35]. In this context, the application in nanohydrometallurgy to recover Rems is strategic as it is considered environmentally friendly. In this methodology, waste is reduced and Nps are reapplied.

A recycling process for phosphogypsum employing nanohydrometallurgy addresses areas such as secondary metal recycling, circular economy, and sustainable development. Consequently, these processes also directly contribute to various Sustainable Development Goals (SDGs) established by the UN for 2030. Therefore, this research aims to investigate the potential and limitations of utilizing nanohydrometallurgy, specifically through the application of functionalized superparamagnetic nanoparticles (Si@FeNps), for the selective separation of Rems from phosphogypsum.

Materials and Methods

Materials

The reagents used for the synthesis of Snps were: Ferric chloride ($FeCl_3{\cdot}6H_2O$), ferrous sulfate ($FeSO_4{\cdot}7H_2O$), tetraethyl orthosilicate (TEOS), ethylenediaminepropyltrimethoxysilane (EAPTMS) and diethylenetriaminepentaacetic anhydride (DTPA), all from Sigma/Aldrich.

The synthesis of solutions with Rems were synthesized using their respective oxides. Cerium(IV) oxide (CeO_2), Dysprosium(III) oxide (Dy_2O_3), Lanthanum(III) oxide (La_2O_3), Neodymium(III) oxide (Nd_2O_3) and Yttrium(III) oxide (Y_2O_3). All from Sigma/Aldrich.

Synthesis of Superparamagnetic Nanoparticles (Snps)

Initially, the synthesis of Snps was achieved through a modified coprecipitation method, adapted from Almeida 2016 [10]. Ferric chloride ($FeCl_3{\cdot}6H_2O$) served as Fe^{3+} sources, while ferrous sulfate ($FeSO_4{\cdot}7H_2O$) provided the Fe^{2+}. The two iron salts were mixed in a basic solution with NH_4OH and an inert atmosphere of N_2. The Snps were coated with silane groups using tetraethyl orthosilicate (TEOS) using a sol–gel process with glycerol and water. Functionalization was performed with ethylenediaminepropyltrimethoxysilane (EAPTMS) and diethylenetriaminepentaacetic anhydride (DTPA).

Recovery of REE with Synthesized Nano Particles

The objectives of this research are to investigate the efficiency and selectivity of superparamagnetic nanoparticles (Si@Fe-DTPA) in the recovery of Rems from synthetic acidic leaching solutions, including monometallic, multimetallic, and phosphogypsum-derived solutions. The study aims to optimize the parameters of temperature and pH. Additionally, the research seeks to propose a process for the recovery of Rems and establish a mass balance for the process.

The nanohydrometallurgy processes used Si@Fe-DTPA in various synthetic acidic leaching solutions for the metals Ce, Dy, La, Nd and Y.

Solutions containing single metals at concentrations of 100, 200, 300, and 400 mg/L were utilized to investigate the solution/Si@Fe-DTPA ratio and the selectivity in monometallic systems. Other parameters tested included the efficiency of metal complexation with Snps at different pH levels (5, 5.5, 6, 6.5, and 7) and complexation efficiency at different temperatures (25, 30, 35, 40, 45, and 50 °C). Temperature was maintained by heat plate. pH of a solution was measured using a Cole-Parmer Combination pH electrode. Metals concentrations in solution were determined by an inductively coupled plasma optical emission spectrometry (ICP-OES, Agilent 5100). Solutions were diluted with 2% nitric acid prior to the analysis.

To investigate selectivity in a multi-metal solution containing Dy, La, Nd, and Y at a concentration of 300 mg/L, a

solution was employed. For the recovery of critical metals from the phosphogypsum compound, a solution with 14 g/L of Ca, 7 mg/L of Ce, 120 mg/L of Dy, 340 mg/L of La, 215 mg/L of Nd, and 660 mg/L of Y was created, adapted from Gao 2019 [36]

For all tests, the pH of the leaching solutions was adjusted to pH 6 using NH_4OH. 50 mL of the pH 6 solution were separated, and 1 g of Si@Fe-DTPA was added for 2.5 h. After this period, the Si@Fe-DTPA nanoparticles were removed using an external magnet. Then, 50 mL of deionized water with pH 2, called new pH 2 solution (adjusted with HNO_3) was added to the Snps for 1.5 h. This methodology was adapted from Pavoski 2024 [3]. All experiments utilized a beaker and a mechanical Teflon stirrer. A schematic of the nanohydrometallurgy process is shown in Fig. 1.

Results and Discussion

Superparamagnetic Nanoparticles: Chemical and Physical Properties

Superparamagnetic nanoparticles (Snps) have gained significant attention due to their unique magnetic behavior, high surface area, and tunable surface chemistry, making them valuable for applications in biomedicine, catalysis, environmental remediation, and metal recovery. Their ability to exhibit magnetism only in the presence of an external field allows for rapid separation, reusability, and process efficiency, distinguishing them from conventional separation materials. Various synthesis routes, including coprecipitation, thermal decomposition, sol–gel, and microemulsion methods, have been developed to control the size, morphology, and surface properties of these nanoparticles. Additionally, functionalization strategies, such as polymer coatings, silica shells, and chelating ligands, further enhance their stability, selectivity, and application potential in complex chemical environments [37–39].

Among the different types of Snps, magnetite-based nanoparticles (Fe_3O_4) have emerged as a prominent choice due to their strong superparamagnetic properties, biocompatibility, and ease of functionalization. In particular, Fe_3O_4 nanoparticles coated with silica (SiO_2) and functionalized with ethylenediaminepropyltrimethoxysilane (EAPTMS) and diethylenetriaminepentaacetic acid (DTPA) have demonstrated high efficiency in selective metal recovery processes, especially for rare earth elements (Rees). The silica shell provides chemical stability and prevents oxidation, while the EAPTMS modification introduces reactive amine groups, allowing further attachment of complexing agents such as DTPA, which plays a crucial role in binding metal ions like Nd^{3+}, La^{3+}, and Y^{3+} [3, 10].

The integration of magnetic separation with selective adsorption makes these Snps highly effective for nanohydrometallurgical applications, as they combine high affinity for metal ions with fast and efficient separation using external magnetic fields. Their colloidal stability, ensured by surface functionalization, minimizes aggregation and enhances reusability over multiple adsorption/desorption cycles, reducing reagent consumption and improving process sustainability. Recent studies indicate that these functionalized Snps achieve over 99% efficiency in metal recovery after multiple reuse cycles, demonstrating their potential as an environmentally friendly alternative to traditional solvent

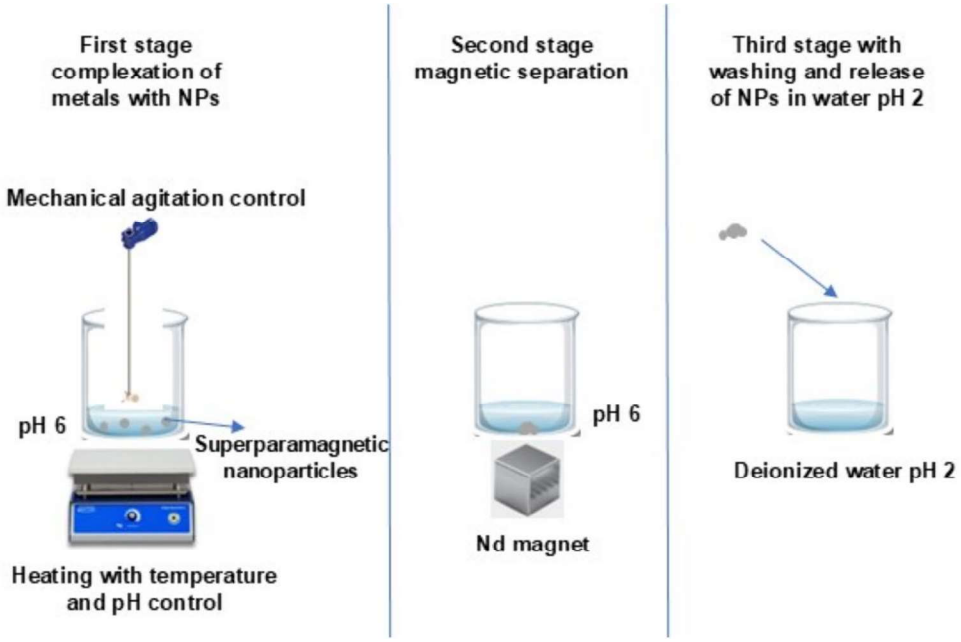

Fig. 1 Stages of the nanohydrometallurgy process for the separation of critical metals, from the complexation of rare earth metals (Rems) in superparamagnetic nanoparticles (Snps) to the release in the new pH 2 solution

extraction and ion exchange methods. Additionally, the ability to fine-tune surface properties allows for customization toward specific target metals, further broadening their applicability in secondary resource recovery and circular economy strategies.

Nanohydrometallurgy for Monometallic Solutions

Tests with different metal concentrations using a set amount of Snps in nanohydrometallurgy are essential for optimizing the recovery efficiency of critical metals. By varying the concentration of the critical metal, it is possible to determine the ideal quantity that maximizes metal adsorption, ensuring efficient resource use and cost reduction. These tests help in understanding the chemical interactions between the Snps and the solution components [12, 40, 41]. Key points include adsorption efficiency, resource economy, chemical equilibrium, separation performance, and Nps reuse. Table 1 shows the separation percentages of Si@Fe-DTPA nanoparticles for different critical metals.

Firstly, it is evident that the results in Table 1 vary according to the metal. This phenomenon can be attributed to the distinct chemical properties of each metal, which significantly influence their interactions during the complexation process with the Snps. Rems are divided into light rare earth elements (Lrees) and heavy rare earth elements (Hrees). Lrees, including elements like Ce, La and Nd, have larger ionic radii and are generally more abundant, with applications in high-performance magnets and catalysts. Hrees, such as Dy and Y, have smaller ionic radii, higher melting points, and are less abundant, often exhibiting superior magnetic and optical properties essential for advanced technologies like lasers and powerful magnets. Dy has an atomic number of 66 and an atomic mass of 162.5 u. La has an atomic number of 57 and an atomic mass of 138.9 u. Nd has an atomic number of 60 and an atomic mass of 144.2 u. Lastly, Y has an atomic number of 39 and an atomic mass of 88.9 u [42].

The complexation process of Rems on Snps involves the binding of metal ions to specific functional groups on the surface, facilitating the separation and recovery of metals. Si@Fe-DTPA nanoparticles possess a large surface area and can be functionalized with various chemical groups. There are two main types of functional groups: cationic and anionic. Examples of cationic functional groups include sulfonic acids ($-SO_3H$) and carboxylic acids (-COOH). The acidic functional groups on the Snps release H^+ ions into the solution, which are replaced by metal cations such as REM^{3+} ions. A general reaction is shown in Eq. 1. In this case, more than one carboxylic acid group is required to complex metals with an oxidation number of + 3. Almeida in 2016 proposed an explanation involving the coordination process between two DTPA molecules. Each DTPA molecule has three protonated amino groups, leaving four carboxylate groups. Thus, the REM can simultaneously bind to two DTPA ligands, achieving a coordination number of 8, which is quite common for lanthanides [10].The availability of different numbers of protonated amino and carboxylate groups are influenced by the size of the ion that will be complexed. With this confirmation, it is possible to better understand the different results in Table 1.

$$R - COOH + REM^{3+} \rightleftarrows R - COOREM + H^+ \quad (1)$$

An example of anionic functional groups are quaternary amines ($-NR_3^+$). Where, the complexation mechanism involves the capture of complex anions from metal ions, such as $[RE(CO_3)_3]^{3-}$, resulting in the capture of this ion from

Table 1 Study of the behavior of Si@Fe-DTPA nanoparticles with different concentrations of critical metal

		100 mg/L		200 mg/L		300 mg/L		400 mg/L	
		Concentration (mg/L)	%	Concentration (mg/L)	%	Concentration (mg/L)	%	Concentration (mg/L)	%
Dy	Synthetic solution	119.32	100.00	219.47	100.00	320.51	100.00	420.43	100.00
	Synthetic solution after the 1st cycle	108.49	90.92	140.11	63.84	196.89	61.43	135.13	32.14
	New solution with pH 2	5.32	4.46	12.11	5.52	18.49	5.77	44.48	10.58
La	Synthetic solution	99.50	100.00	198.97	100.00	299.76	100.00	398.69	100.00
	Synthetic solution after the 1st cycle	88.46	88.90	162.56	81.70	247.90	82.70	365.60	91.70
	New solution with pH 2	17.21	17.30	22.28	11.20	53.06	17.70	22.33	5.60
Nd	Synthetic solution	98.78	100.00	197.97	100.00	289.26	100.00	392.29	100.00
	Synthetic solution after the 1st cycle	30.36	30.74	63.29	31.97	152.24	52.63	206.46	52.63
	New solution with pH 2	20.36	20.61	34.03	17.19	64.33	22.24	88.30	22.51
Y	Synthetic solution	97.63	100.00	199.48	100.00	293.54	100.00	397.51	100.00
	Synthetic solution after the 1st cycle	88.77	90.92	179.25	89.86	270.67	92.21	349.69	87.97
	New solution with pH 2	4.35	4.46	9.12	4.57	18.35	6.25	10.57	2.66

the solution. A global example is shown in Eq. 2. Thus, depending on the functional group attached to the Snps, there will be varying degrees of affinity for specific metals, maintaining selectivity. In studies involving ion exchange resins, this order of selectivity has been extensively verified, as referenced by Vinco's research in 2022 [43, 44]. However, the selectivity for Snps has not yet been studied, creating a precedent for this research.

$$R-NR_3OH+\left[RE(CO_3)_3\right]^{3-} \rightleftharpoons R-NR_3\left[RE(CO_3)_3\right]+3OH^- \quad (2)$$

In solutions with only one metal, Nd showed the highest transfer percentage to the new pH 2 solution, as well as the greatest reduction in the metal concentration in the initial solution. The new pH 2 solution obtained approximately 21% of the Nd mass in one cycle at different initial concentrations. It can be noted that Nd is known for its strong magnetic properties, and the functionalization of Snps can leverage this characteristic, forming stable complexes due to their size coordinating with the protonated amino and carboxylate groups and increasing capture efficiency in aqueous solutions.

On the other hand, Y exhibited the lowest transfer percentage in one cycle of nanohydrometallurgy. This low percentage can be discussed since this metal has the lowest atomic mass, which may result in less stable complexes compared to the other metals. However, its specific chemical and physical properties still allow the formation of complexes, even if it does not complex with all available protonated amino and carboxylate groups. Finally, in the test with single-metal solutions at varying concentrations, the selectivity order of the metals for Si@Fe-DTPA followed the trend Nd > La > Dy > Y, which correlates with differences in ionic radius, coordination chemistry, and electrostatic interactions. The results for metal complexation capacity per gram of Si@Fe-DTPA are presented in Table 2, demonstrating that complexation efficiency increases with metal transfer. The maximum complexation capacities were Nd (90.04 mg/g), La (53.10 mg/g), Dy (42.30 mg/g), and Y (10.64 mg/g). This trend aligns with the distinction between Lrees and Hrees. Lrees, such as Nd and La, have larger ionic radii (Nd^{3+} = 0.983 Å, La^{3+} = 1.032 Å), which facilitates higher binding affinity with DTPA due to greater accessibility to chelating sites and steric factors that enhance coordination stability. In contrast, Hrees, such as Dy and Y, exhibit smaller ionic radii (Dy^{3+} = 0.912 Å, Y^{3+} = 0.900 Å) and higher charge density, leading to stronger hydration energy and reduced accessibility to the chelating ligand, which lowers their complexation efficiency. Additionally, Ce was tested under the same conditions, but at the analyzed concentrations, it precipitated at pH 6, likely due to oxidation to Ce^{4+} and subsequent hydrolysis, forming insoluble $Ce(OH)_4$. These findings emphasize that metal size, charge density, and hydration energy play crucial roles in determining the complexation efficiency of Si@Fe-DTPA, reinforcing its high selectivity for Nd^{3+} and La^{3+} over Dy^{3+} and Y^{3+}.

Table 2 Results of the maximum transfer capacity of Dy, La, Nd, and Y metals shown in mg of metal per g of Si@Fe-DTPA

Concentration\ metal	Dy (mg Dy/g Nps)	La (mg La/g Nps)	Nd (mg Dy/g Nps)	Y (mg Dy/g Nps)
100 mg/L	5.76	17.30	20.61	4.46
200 mg/L	11.04	22.40	34.38	9.14
300 mg/L	17.31	53.10	66.72	18.75
400 mg/L	42.30	22.40	90.04	10.64

The significantly higher complexation capacities obtained in this study, with Nd at 90.04 mg/g and La at 53.10 mg/g, compared to 62 mgLa/gNP and 28 mgNd/gNP in Almeida (2016) [10] and 1.8 mgLa/gNP in Pavoski (2024) [3], highlight the impact of synthetic modifications on adsorption efficiency. The use of an inert atmosphere during synthesis minimized Fe_3O_4 oxidation, preserving its superparamagnetic properties and enhancing metal adsorption. Additionally, increasing complexation time allowed greater interaction between the metal ions and DTPA-functionalized binding sites, leading to higher recovery. Structural differences, including a more uniform nanoparticle size and a higher surface area, provided greater ligand availability and adsorption capacity, particularly favoring Lrees (Nd^{3+}, La^{3+}) over Hrees (Dy^{3+}, Y^{3+}) due to their larger ionic radii and enhanced accessibility to chelating sites. These findings highlight how slight modifications in synthesis, including controlled oxidation, precise adjustment of reaction conditions, and ligand functionalization, have a direct impact on selectivity and adsorption efficiency. Given the strong dependence of SNP efficiency on synthesis parameters, ensuring replicability and standardization is essential for advancing scalable and sustainable nanohydrometallurgical processes.

Currently, there are no scientific studies available on the concentration of Dy and Y in nanohydrometallurgy. However, we can reference other metals. The values for Dy at 42.30 mg/gNps are higher, and Y at 10.64 mg/gNps are lower than those reported for Au and Li in Mattioni in 2022 study [11], which showed a value of 32.6 mg Au/g Fe_3O_4, and Quartarolli in 2022 study [45], which reported 30.2 mg Li/g(magnetic composite). This comparison highlights that all the metals and Snps involved are different, confirming that each process in nanohydrometallurgy is unique. It will always depend on the functional groups attached to the Nps, whether they are cationic or anionic, as well as on the metal of interest, considering its size and oxidation state. The first consideration in these processes is to confirm whether the initial leaching solution containing the metals of interest can

undergo pH changes without precipitating the metal of interest or other metals. This can positively or negatively impact the nanohydrometallurgy process, affecting the percentage of metal transfer. This step can facilitate selective recovery processes if the precipitation of an undesired metal occurs, such as in the recovery of La from spent catalysts where pH changes precipitate Al. Conversely, pH changes can hinder nanohydrometallurgy if the metal of interest precipitates.

Another critical factor is the composition of the Snps in terms of functionalization (complexing functional groups), which can affect complexation. Different metals have different sizes and oxidation states, as observed with Dy, Y, Au, and Li. These metals are more or less selective to different functional groups such as carboxylic acids, amines (primary, secondary, and tertiary), iminodiacetic acid (IDA), bis-picolylamine, and sulfonic acid. According to results with Rems, protonated amino and carboxylate groups are selective for Rems. This selectivity will depend on the number of active sites capable of releasing H^+, being sufficiently electronegative, and forming the Nps-Rems complex.

The graph in Fig. 2a, with initial concentration on the X-axis and complexation percentage on the Y-axis, is crucial in nanohydrometallurgy for evaluating the efficiency of metal complexation processes. It is observed that the different lines for various metals show different behaviors, with the lines for Nd and Dy above others, indicating higher efficiency in complexation. This graph helps determine how complexation efficiency varies with different initial concentrations, identify the optimal concentration that maximizes complexation, and optimize reagent usage. Another important aspect is whether the lines exhibit a linear or nonlinear trend. A linear relationship may indicate that complexation is directly proportional to the initial concentration up to a certain point. A nonlinear relationship may indicate phenomena such as saturation or equilibrium effects, where the complexation rate decreases or stabilizes beyond a certain point. For La and Y, the relationship is linear, while for Dy, it is nonlinear. Dy complexation remains constant up to a concentration of 300 mg/L and decreases thereafter. Conversely, for Nd, the nonlinear effect shows lower complexation at concentrations below 200 mg/L, increasing thereafter. An important fact to discuss is that the percentage of complexation is different from the percentage of transfer. These two percentages need to be discussed together. The best processes exhibit equal percentages. If this number is not equal, there may be losses in the washing processes, resulting in a lower transfer percentage. Therefore, it is necessary to study the washing water or recycle it to avoid metal losses.

The data presented in Fig. 2b, with the X-axis representing the percentage of metal complexation and the Y-axis representing the percentage of extraction (stripping) into a new solution, is essential for evaluating and optimizing the metal extraction process. This graph helps determine how metal complexation in the initial solution affects the efficiency of metal stripping into a new solution. It identifies the optimal percentage of complexation that maximizes metal extraction, allowing for the optimization of reagent usage and operational conditions such as concentration, pH, and temperature. Furthermore, it reveals whether the relationship between complexation and extraction is linear or shows saturation or equilibrium phenomena, indicating potential inefficiencies or limitations in the stripping process. The graph demonstrates that, for all four metals, the relationship is nonlinear. The best complexation and extraction efficiencies are observed for La, as nearly all the complexed metal is extracted into a new solution. Nd follows as the second-best, while Dy and Y rank third and fourth, respectively. The data suggest that Dy and Nd exhibit the highest levels of complexation, but their extraction percentages decrease, indicating losses during the washing processes. Therefore, it is necessary to recycle the washing water for these metals to minimize losses.

According to in Fig. 2c, with the X-axis representing the metal concentration in the synthetic solution after the first cycle (in mg/L) and the Y-axis representing the specific metal complexation (in mg/g), is essential for evaluating and optimizing the metal extraction process. It assesses the efficiency of the complexing agent in capturing the metal and allows for the adjustment of process conditions. This graph can indicate whether there is a direct relationship where higher metal concentration leads to increased specific complexation or if a saturation point is reached where complexation levels off. It also provides insights into the capacity of the complexing agent and the overall efficiency of the process, guiding adjustments in operational parameters to achieve optimal metal recovery. The behavior of the lines varied among the metals. Nd showed a linear trend with increasing loading capacity of Si@Fe-DTPA at different concentrations. Thus, Nd demonstrated that as complexation decreases (when the concentration in the synthetic solution remains high), the specific complexation of the metal increases. This suggests greater availability of Nd in more concentrated solutions, resulting in higher specific complexation. In contrast, metal Y exhibited a linear trend but with consistently lower specific complexation compared to other metals, reflecting the effect of concentration differences in the synthetic solution. For La and Dy, no clear trend was observed, with distinct behaviors for each metal.

Analyzing Fig. 2d, with the X-axis representing the initial metal concentration (in mg/L) and the Y-axis representing the metal concentration in the synthetic solution after the 1st cycle (in mg/L), is crucial for assessing and optimizing the metal separation and purification process. This graph illustrates how the initial metal concentration in the solution impacts its concentration in the raffinate after the separation process. It can reveal whether there is a linear relationship,

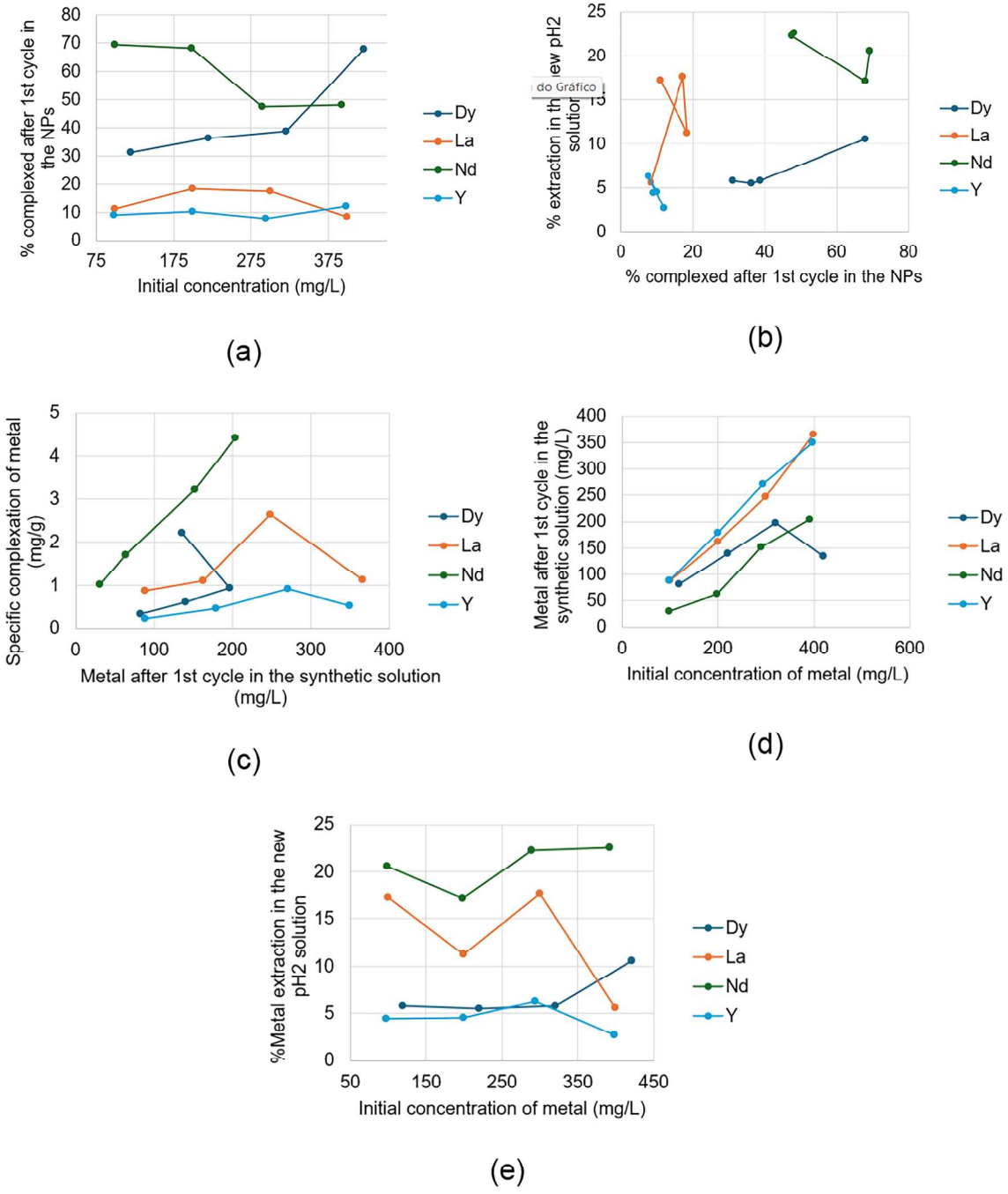

Fig. 2 Graphs representing the different results obtained with the nanohydrometallurgy tests for the metals Dy, La, Nd and Y. **a** Initial concentration (mg/L) by % of nanoparticle complexation. **b** % of nanoparticle complexation by % of extraction to new pH 2 solution. **c** concentration of metals after 1st cycle in the synthetic solution (mg/L) by specific complexation (mg/g). **d** Initial concentration (mg/L) by concentration of metals after 1st cycle in the synthetic solution (mg/L). **e** Initial concentration (mg/L) by % of extraction to new pH 2 solution

where the raffinate concentration increases proportionally with the initial concentration, or if there are nonlinear effects, such as saturation. The graph also provides insights into the process's capacity to handle varying initial metal concentrations and highlights any operational limitations or inefficiencies. For La, Nd, and Y, a linear relationship is observed, suggesting that the separation process is effective and that the metal removal capacity is directly proportional to the initial concentration, in this case the value to be observed and compared is also that of specific complexation

of each metal in mg of metal per g of Si@Fe-DTPA. This implies that adjusting process conditions to achieve desired efficiency may be more straightforward. However, for Dy, the relationship becomes nonlinear at concentrations above 300 mg/L. This nonlinearity indicates that the separation process may face limitations at higher concentrations, such as system saturation or the limited capacity of Si@Fe-DTPA. Consequently, adjustments to the process may be required.

Observations from Fig. 2e, with the X-axis representing the initial metal concentration (in mg/L) and the Y-axis representing the percentage of stripping into a new solution, is crucial for assessing and optimizing the metal recovery process. In this graph, it is possible to observe that the highest extraction percentage results were for the metal Nd, with values ranging from 20 to 23%. In second place comes La, with higher extraction percentages for concentrations below 300 mg/L. The metals Dy and Y, in concentrations below 300 mg/L, showed the same trend, and in higher concentrations Dy stands out, increasing its concentration percentage. Thus, showing that to transfer Dy, solutions with concentrations above 300 mg/L are preferential.

Complexation Behavior at Different pHs and Temperatures

Analyzing the nanohydrometallurgy process at different pH levels and temperatures is crucial for optimizing the efficiency and selectivity of Rems recovery. The pH affects the protonation state of functional groups on the nanoparticles, such as carboxylic acids and amines, altering their charge and ability to complex with metal ions. At higher pH, carboxylic groups deprotonate, forming carboxylates ($–COO^-$), which can bind metal cations, while amines deprotonate at lower pH, forming neutral amines. Temperature influences the system's entropy, with higher temperatures increasing kinetic energy and the disorder of ions and functional groups, facilitating complex formation. The release of protons during deprotonation increases system entropy, making complexation thermodynamically favorable. The results of the nanohydrometallurgy tests at different pH levels and temperatures for the metals Dy, La, Nd, and Y are shown in Fig. 3.

Observing the pH variation in Fig. 3a, it is possible to notice a consistency in the metal transfer results within the pH range of 5.5 to 7. However, for pH values below 5.5, there was inefficiency in metal complexation, causing the value to drop. At this pH, the deprotonation of the amino and carboxylate groups is not favored. Therefore, the region with negative density does not occur to complex with the ion of the positive Rems. This parameter can influence metal speciation. For example, certain metals can be in the form of free ions in acidic pH, while in neutral or basic pH they may precipitate or form different complexes. Another factor is the surface charge of the Snps, which is also affected by pH. The functionalization of nanoparticles depends on functional groups that can protonate or deprotonate depending on the pH. In the case of Si@Fe-DTPA, it is necessary to deprotonate the carboxylic acid groups on the surface. Regarding metal solubility, pH can also interfere. In lower transfer values, this factor may be occurring for Si@Fe-DTPA, since tests could not be performed with the metal Ce. Finally, pH below 5.5 may be impairing the stability of the complexes (Si@Fe-DTPA-metal) [10, 11, 14, 45, 46]

The results related to Fig. 3b show a consistency in the metal transfer results at different temperatures in the nanohydrometallurgy processes. This indicates that temperature does not influence in complexation reactions, and room temperature is strategic to reduce the process energy costs.

Nanohydrometallurgy for Multimetallic and Phosphogypsum Solutions

To investigate selectivity in a multi-metal solution with Ce, Dy, La, Nd, and Y metals at a concentration of 300 mg/L was employed. Table 3 presents the results of metal concentrations (Dy, La, Nd, and Y) in a synthetic multi-metal solution after the first cycle of nanohydrometallurgy, and the subsequent metal transfer to a new solution of pH 2. The table details the removal efficiency of each metal by the functionalized Si@Fe-DTPA and the amount of metal transferred to the acidic solution.

The results presented in Table 3 demonstrate the variation in metal concentrations after the first treatment cycle with Snps and the subsequent transfer to a new solution with pH 2. It is possible to observe that the removal efficiency varies significantly among different metals, with Dy showing the highest reduction in concentration (41.93%), while La had the lowest reduction (8.16%). These data indicate that the specific chemical properties of each metal strongly influence their ability to form stable complexes and differ from single-metal solutions and multi-metal solutions, consequently affecting their removal efficiency.

However, the analysis of the metal concentrations in the new pH 2 solution reveals that the metal with the highest transfer percentage to this solution was Y (12.71%), followed by Nd (10.64%). Interestingly, Dy, which showed the highest reduction in the initial solution after the first cycle, did not have the highest concentration in the pH 2 solution, with only 3.47% transfer. This suggests that during the Snps washing process, there may be a loss of this metal, affecting the accuracy of the final results. This possibility of loss during washing is a critical factor to consider. This phenomenon may occur due to incomplete adhesion of the metal complexes to the nanoparticles or partial removal of the metals during the process due to instability.

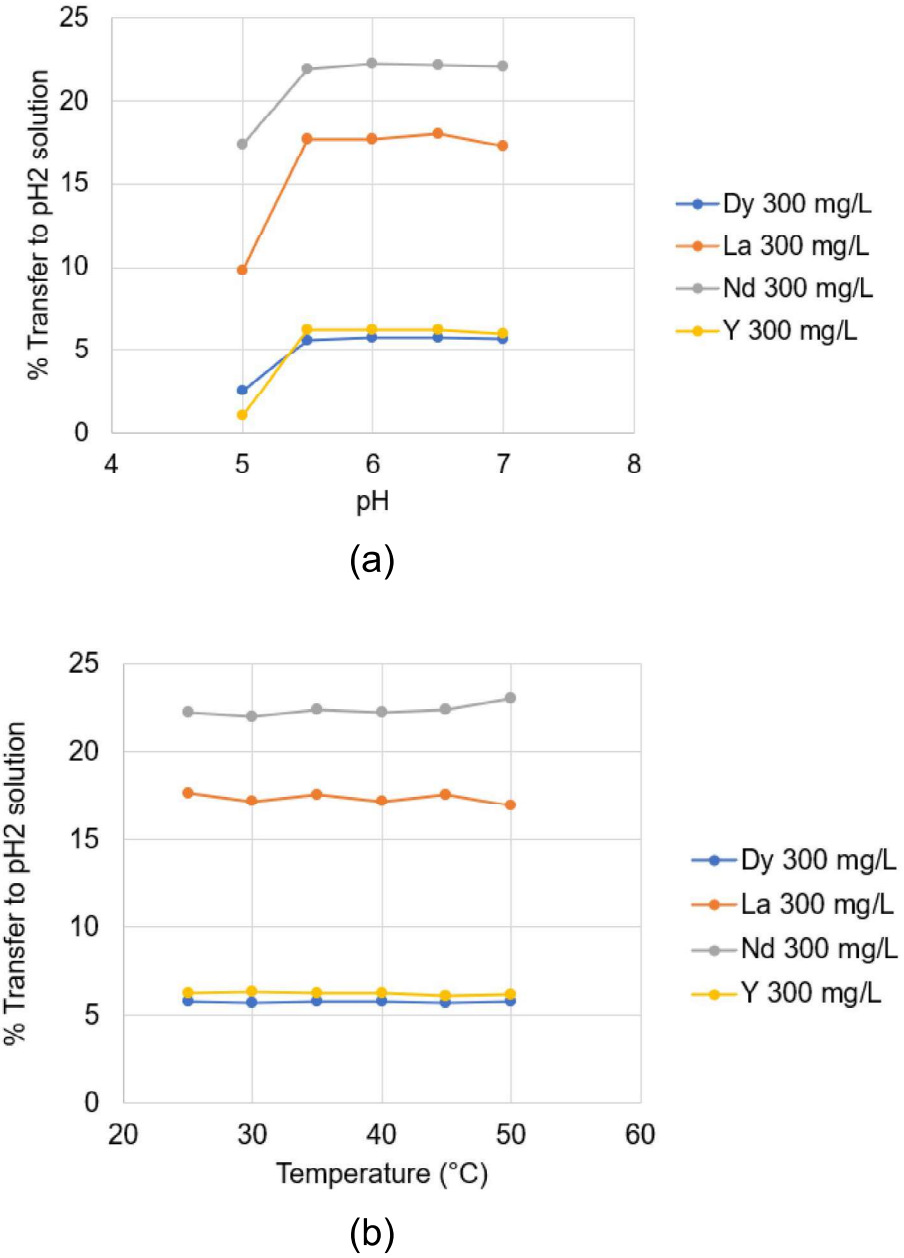

Fig. 3 Results of nanohydrometallurgy tests for Dy, La, Nd, and Y metals varying pH and temperature parameters using a synthetic solution with only one metal. **a** pH variation in the range of 5–7. **b** Temperature variation in the range of 25–50 °C

Table 3 Concentrations of metals in synthetic multi-metal solutions after the first cycle of nanohydrometallurgy with transfer to a solution of pH 2

	Dy		La		Nd		Y	
	(mg/L)	(%)	(mg/L)	(%)	(mg/L)	(%)	(mg/L)	(%)
Multimetal synthetic solution	390.84	100.00	381.13	100.00	320.25	100.00	379.85	100.00
Synthetic multimetal solution after the 1st cycle (a)	226.95	41.93	350.01	8.16	239.05	25.36	249.59	34.29
New solution with pH 2 (b)	13.55	3.47	16.68	4.38	34.06	10.64	48.27	12.71

(a) % loss, (b) % transfer

The selectivity order of Si@Fe-DTPA for metal adsorption, Nd > Y > La > Dy, is strongly influenced by the chemical properties of each element, including ionic radius, charge density, ligand affinity, and their ability to form coordination complexes with a coordination number of 8. The extraction percentages at pH 2, where Nd (10.64%) and Y (12.71%)

exhibit similar retention, suggest that these metals form the most stable complexes with the functionalized nanoparticles. Nd^{3+} (0.983 Å) and Y^{3+} (0.900 Å) possess ideal ionic radii and coordination behavior, enhancing their interaction with the carboxylate ($–COO^-$) and amine ($–NH_2$) groups of the DTPA ligand. La^{3+} (1.032 Å), despite its structural similarity to Nd, shows lower complexation due to its larger size and reduced electrostatic attraction, while Dy^{3+} (0.912 Å), with its higher charge density and stronger hydration energy, faces steric hindrance that limits efficient binding. The preference for metals that adopt a coordination number of 8 aligns with the structural requirements of the DTPA ligand, further influencing selectivity. These results highlight that the coordination environment of each metal dictates its interaction with Snps, reinforcing the importance of controlled synthesis and process optimization. Adjusting pH levels, SNP dosage, and contact time can further enhance selectivity, ensuring a more efficient and scalable approach for rare earth element recovery in complex metal solutions.

Table 4 presents the results of the recovery of critical metals from phosphogypsum using the nanohydrometallurgy process. This material is a by-product of phosphoric acid production from phosphate rock and contains several metals of industrial interest, including rare earth elements studied in this research (Ce, Dy, La, Nd, and Y). The results detail the concentrations of these metals in the initial phosphogypsum solution and the amounts recovered after treatment with Si@Fe-DTPA, highlighting the efficiency of the recovery process.

Research on the recovery of critical metals from phosphogypsum is of great importance due to the growing demand for these elements in various technological and industrial applications. Metals such as Nd and Dy are essential for the manufacture of permanent magnets used in electric motors and wind turbines, while La and Ce are used in catalysts and special alloys. Recycling and recovering these metals from industrial waste not only helps reduce dependence on primary sources, often scarce and geographically concentrated, but also contributes to environmental sustainability by minimizing the amount of hazardous waste.

Table 4 presents the concentrations of different metals in a synthetic phosphogypsum solution and their values after the first cycle of nanohydrometallurgy and transfer to a new pH 2 solution. Analyzing the nanohydrometallurgy procedure, it can be observed that calcium (Ca), the element with the highest concentration, is the first to be separated from the critical metals, followed by the individual separation of the critical metals [10, 13, 31]. This is possible because a selectivity order of Si@Fe-DTPA for multi-metal solutions was observed. The results for Ca were promising, as only a small fraction was transferred to the new pH 2 solution. This demonstrates that this fraction is due to the high initial concentration (14,286.71 mg/L of Ca) and that the Snps do not complex Ca, allowing the critical metals to be separated in the second cycle.

The critical metals showed considerable reduction in concentration and transfer. For Ce, 17.59% was transferred to the new pH 2 solution; Dy had a transfer percentage of 5.96%; La had a transfer of 13.74%; Nd transferred 19.83%; and Y achieved a transfer of 12.93% to the new solution.

It is possible to estimate the number of cycles needed to obtain solutions with only one metal by consistently applying the same transfer percentage. For example, Ce had a transfer of 17.59% to the new solution after one cycle, suggesting that approximately six cycles would be needed. For Dy, which had a transfer of 5.96% after the first cycle, approximately 17 cycles would be required to achieve significant separation. La, with a transfer of 13.74%, would need about seven cycles to be effectively separated. Nd, with a transfer of 19.83%, would require approximately five cycles. Finally, Y, with a transfer of 12.93%, would need about eight cycles to achieve efficient separation. These cycle estimates can be considered even though the percentages tend to change with concentration changes. However, as the solutions become more diluted, the transfer percentage of critical metals tends to increase, thus potentially reducing the projected number of cycles.

The proposed mass balance for the nanohydrometallurgy of 1000 L of a phosphogypsum leaching solution is shown in Fig. 4. The flowchart shows the results of the separation of critical metals in the first three cycles.

The nanohydrometallurgy process, as shown in Fig. 4, demonstrates a progressive mass transfer of the target elements (Ce, Dy, La, Nd, Y) into the new pH 2 solution over

Table 4 Recovery of critical metals from a synthetic leach solution of phosphogypsum using nanohydrometallurgy

	Ca		Ce		Dy		La		Nd		Y	
	(mg/L)	(%)	(mg/L)	(%)	(mg/L)	(%)	(mg/L)	(%)	(mg/L)	(%)	(mg/L)	(%)
Multimetal synthetic solution	14,286.72	100	6.27	100	118.45	100	335.18	100	217.41	100	652.82	100
Synthetic multimetal solution after the 1st cycle (a)	11,981.74	16.13	3.61	42.42	68.03	42.57	257.93	23.05	136.67	37.14	468.09	28.30
New solution with pH 2 (b)	64.71	0.45	1.10	17.59	7.06	5.96	46.05	13.74	43.11	19.83	84.44	12.93

(a) % loss, (b) % transfer

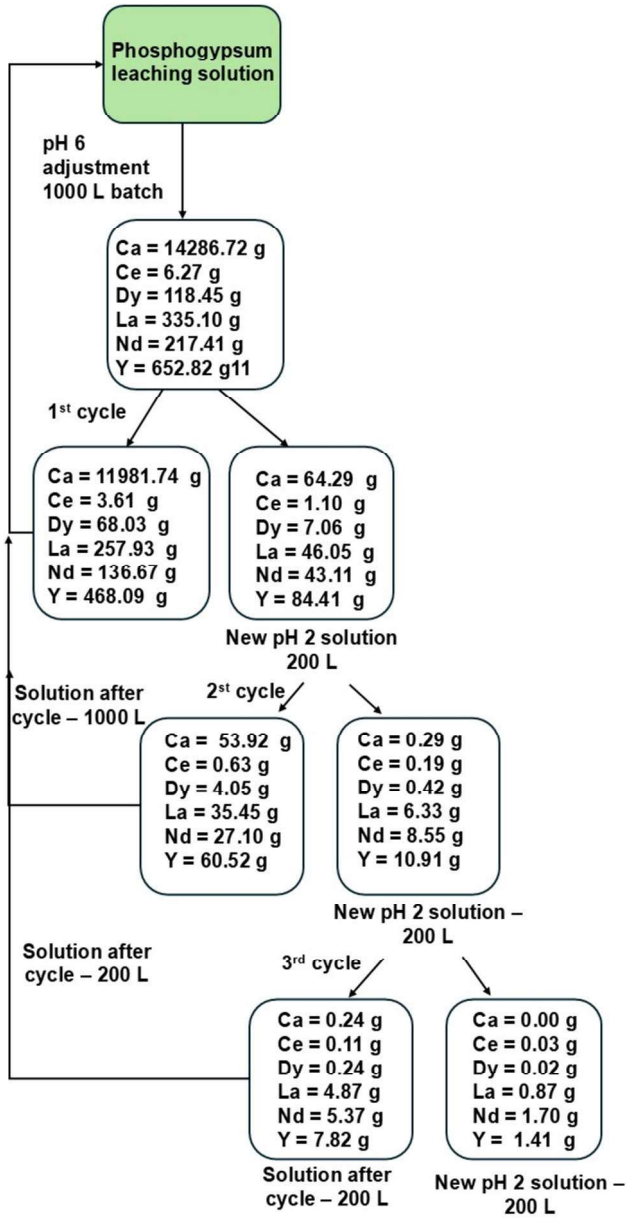

Fig. 4 Proposed mass balance for the first three nanohydrometallurgy experiments of 1000 L of a phosphogypsum leaching solution

three leaching cycles. Initially, the leaching solution contained significant concentrations of these elements: Ca (14,286.72 g), Ce (6.27 g), Dy (118.45 g), La (335.10 g), Nd (217.41 g), and Y (652.82 g). An important point is the transfer of Ca in the first cycle, which can be attributed to its initial concentration. After three cycles of nanohydrometallurgy, Ca was no longer detected, indicating that Si@Fe-DTPA is selective for Rems and not selective for Ca.

In the first cycle, following the transfer, the pH2 solution had the following concentrations: Ca (64.29 g), Ce (1.10 g), Dy (7.06 g), La (46.05 g), Nd (43.11 g), and Y (84.41 g). The reduction in concentrations in the leaching solution (now referred to as the raffinate) demonstrates the mass transfer to the pH2 solution. For instance, calcium (Nd) decreased from 217.41 g to 136.67 g in the raffinate, while in the pH2 solution, it increased to 43.11 g.

In this part of the process, two key methodological paths can be highlighted. The first involves studying the volume of the new pH 2 solution. This volume can be adjusted, which would modulate the concentration of the solution and potentially reduce the amount of reagents used. In this process, 200 L of deionized water with pH2 was selected for extraction. The second point concerns the raffinate solution. This solution can be returned and mixed with the initial leaching solution to avoid discarding valuable metals. Additionally, the washing solution can also be recycled to the beginning of the process. These steps are feasible because, even though the initial solution is diluted by returning more solutions, the selectivity of Si@Fe-DTPA ensures the extraction of Rems.

By the third cycle, it is evident that the critical metals have been separated from Ca, with the concentration in the raffinate decreasing further: Ca (0.24 g), Ce (0.11 g), Dy (0.24 g), La (4.87 g), Nd (5.37 g), and Y (7.82 g). The new pH 2 solution showed minimal values, with Ca (0.00 g), Ce (0.03 g), Dy (0.02 g), La (0.87 g), Nd (1.70 g), and Y (1.41 g), confirming that the majority of critical metals were extracted over the cycles.

Ce is a metal that must be discussed in all processes involving nanohydrometallurgy. Due to its concentration, Ce was separated in the phosphogypsum solution; however, in tests with varying concentrations in monometallic solutions, it precipitated. Thus, the pH change in the leaching solution causes metals to precipitate. This also occurs with Al, as reported by Pavoski in 2024[3], where aluminum precipitated. Therefore, all processes need to be thoroughly studied, from leaching and pH adjustment to separation with Snps. Depending on the metals involved, the process needs to be adjusted. This opens perspectives for nanohydrometallurgy to be applied to other residues or might necessitate changing the Snps if its use is not feasible.

The objectives of the UN Sustainable Development Goals (SDGs) 9, 12, and 13 are closely linked with the nanohydrometallurgy of phosphogypsum [47–49]. SDG 9 focuses on building resilient infrastructure, promoting inclusive and sustainable industrialization, and fostering innovation. By utilizing nanohydrometallurgy, we can develop innovative techniques for recovering critical metals from industrial by-products like phosphogypsum, thus contributing to sustainable industrial practices. SDG 12 emphasizes responsible consumption and production, and nanohydrometallurgy aligns with this goal by promoting the efficient use of resources and minimizing waste through the recovery and recycling of valuable metals. Lastly, SDG 13 calls for urgent action to combat climate change and its impacts. By implementing sustainable metal recovery processes,

nanohydrometallurgy reduces the environmental footprint associated with mining and metal extraction, thereby contributing to climate action. In summary, the application of nanohydrometallurgy in processing phosphogypsum supports the advancement of these key SDGs, promoting sustainability and environmental stewardship.

Conclusion

This study demonstrated that nanohydrometallurgy using superparamagnetic nanoparticles (Si@Fe-DTPA) is an efficient and sustainable approach for selectively recovering critical metals from complex solutions, including synthetic monometallic, multimetallic, and phosphogypsum leachates. The process achieved a high selectivity order of Nd > Y > La > Dy > Ce, with maximum adsorption capacities of Nd (90.04 mg/g) and La (53.10 mg/g), significantly surpassing previous studies. The optimized synthesis conditions, including inert atmosphere processing and extended complexation times, contributed to these improved recovery rates. Additionally, the removal of Ca, the primary contaminant, in three cycles highlights the viability of this method for multi-cycle metal separation.

The efficiency of nanohydrometallurgy is influenced by several key factors, including the availability of active functional groups ($-COO^-$, $-NH_2$) on Snps, pH-dependent stability of metal complexes, and metal competition in multimetallic solutions, all of which impact selectivity and adsorption capacity. The process benefits from modifications in SNP synthesis, which enhance magnetic properties, surface area, and ligand interaction, ensuring superior metal recovery compared to conventional solvent extraction and ion exchange methods.

Further research is needed to optimize parameters such as metal concentration, pH control, and SNP dosage for industrial scalability. Exploring alternative functionalization strategies and integrating automated magnetic separation systems could further enhance efficiency and reduce costs.

From a sustainability perspective, this study aligns with SDG 9 (Industry, Innovation, and Infrastructure), SDG 12 (Responsible Consumption and Production), and SDG 13 (Climate Action) by promoting resource efficiency, reducing reliance on primary mining, and advancing circular economy principles.

In conclusion, nanohydrometallurgy presents a promising step toward more efficient, selective, and environmentally responsible metal recovery. Continued research and process optimization will be essential for transitioning from laboratory-scale studies to large-scale industrial applications, ensuring a sustainable and resilient supply of critical materials for modern technologies.

Acknowledgments The authors would like to thank the financial support. Grant 2019/11866-5 (thematic project), 2021/15156-2 and 2023/01064-4 São Paulo Research Foundation (FAPESP).

Declarations

Conflict of interest The authors declare that they have no known competing financial interests or personal relationships that could have appeared to influence the work reported in this paper.

References

1. Chong S, Riley BJ, Lu X et al (2024) Synthesis and properties of anhydrous rare-earth phosphates, monazite and xenotime: a review. RSC Adv 14:18978–19000. https://doi.org/10.1039/d4ra01142b
2. Pavoski G, Garjulli F, Renato dos Santos C et al (2022) Synthesis of a magnetic composite of silica with micro and nano-cobalt metallic structures from a spent catalyst (Co3O4). Mater Sci Eng B 285:115921. https://doi.org/10.1016/j.mseb.2022.115921
3. Pavoski G, Toma HE, Espinosa DCR, Tenório JAS (2024) Nanohydrometallurgy with superparamagnetic nanoparticles for selective separation of lanthanum from a real spent catalyst. J Mater Cycles Waste Manag. https://doi.org/10.1007/s10163-024-02020-7
4. Marinato Y, Pavoski G, Rosario CGA et al (2023) Ag recovery from waste printed circuit boards of cell phone for synthesis of Ag nanoparticles and their antibacterial activity. J Mater Cycles Waste Manag. https://doi.org/10.1007/s10163-022-01579-3
5. Zou J, Zhang R, Zhang Y et al (2024) Extraction of organic solvents and preferential recovery of lithium from spent lithium-ion batteries by in-situ carbothermal reduction. Process Saf Environ Protect 187:259–269. https://doi.org/10.1016/j.psep.2024.04.133
6. Tee KA, Badsha MAH, Khan M et al (2022) Lanthanum carbonate nanoparticles confined within anion exchange resin for phosphate removal from river water: batch and fixed-bed column study. Process Saf Environ Protect 159:640–651. https://doi.org/10.1016/j.psep.2022.01.008
7. Cui L, Yliniemi K, Vapaavuori J, Lundström M (2023) Recent developments of electrodeposition-redox replacement in metal recovery and functional materials: a review. Chem Eng J 465:142737. https://doi.org/10.1016/j.cej.2023.142737
8. Solberg SBB, Gómez-Coma L, Wilhelmsen Ø et al (2024) Electrodialysis for efficient antisolvent recovery in precipitation of critical metals and lithium-ion battery recycling. Chem Eng J 486:150281. https://doi.org/10.1016/j.cej.2024.150281
9. Espinosa DCR, de Oliveira RP, Martins TAG (2022) Recycling Technologies – Hydrometallurgy. In: Holuszko ME, Amit K, Denise CRE (eds) Electronic Waste Recycling and Reprocessing for a Sustainable Future. Wiley, Hoboken, pp 165–187
10. Almeida SDN, Toma HE (2016) Neodymium(III) and lanthanum(III) separation by magnetic nanohydrometallurgy using DTPA functionalized magnetite nanoparticles. Hydrometallurgy 161:22–28. https://doi.org/10.1016/j.hydromet.2016.01.009
11. Mattioni JV, Franciscato DS, Melo FM et al (2022) Nanohydrometallurgical extraction of gold based on ranelate induced nanoparticles formation. Hydrometallurgy 213:105936. https://doi.org/10.1016/j.hydromet.2022.105936
12. Toma HE (2015) Magnetic nanohydrometallurgy: a nanotechnological approach to elemental sustainability. Green Chem 17:2027–2041. https://doi.org/10.1039/c5gc00066a

13. de Melo FM, Almeida SN, Toma HE (2020) Magnetic Nanohydrometallurgy Applied to Lanthanide Separation. Minerals (Basel) 10:530. https://doi.org/10.3390/min10060530
14. Almeida SDN, Toma HE (2019) Lanthanide ion processing from monazite based on magnetic nanohydrometallurgy. Hydrometallurgy. https://doi.org/10.1016/j.hydromet.2019.105138
15. Merroune A, Ait Brahim J, Achiou B et al (2024) Closed-loop purification process of industrial phosphoric acid: selective recovery of heavy metals and rare earth elements via solvent extraction. Desalination 580:117515. https://doi.org/10.1016/j.desal.2024.117515
16. Drogobuzhskaya S, Frolova M, Shishov A, Tsvetov N (2024) Comparison of extraction abilities of deep eutectic solvents and aqueous acid solutions for extraction of rare earths and transition metals. J Rare Earth 42:1157–1164. https://doi.org/10.1016/j.jre.2023.06.014
17. Yu G, Ni S, Gao Y et al (2024) Recovery of rare earth metal oxides from NdFeB magnet leachate by hydrophobic deep eutectic solvent extraction, oxalate stripping and calcination. Hydrometallurgy 223:106209. https://doi.org/10.1016/j.hydromet.2023.106209
18. Hermassi M, Granados M, Valderrama C et al (2022) Impact of functional group types in ion exchange resins on rare earth element recovery from treated acid mine waters. J Clean Prod 379:134742. https://doi.org/10.1016/j.jclepro.2022.134742
19. Roa A, López J, Cortina JL (2024) Recovery of Rare Earth Elements from Acidic Mine Waters: a circular treatment scheme utilizing selective precipitation and ion exchange. Sep Purif Technol 338:126525. https://doi.org/10.1016/j.seppur.2024.126525
20. El Ouardi Y, Virolainen S, Massima Mouele ES et al (2023) The recent progress of ion exchange for the separation of rare earths from secondary resources – a review. Hydrometallurgy 218:106047. https://doi.org/10.1016/j.hydromet.2023.106047
21. Xing M, Wu X, Li Z et al (2023) Rare earth element recovery and aluminum-rich residue production from high alumina fly ash by alkali pre-desilication enhance the mechanochemical extraction process. Process Saf Environ Protect 175:60–69. https://doi.org/10.1016/j.psep.2023.05.022
22. Liu C, Luo W, Liu Z et al (2022) Microwave absorption properties of spent green phosphor and enhanced extraction of rare earths. Process Saf Environ Protect 162:395–405. https://doi.org/10.1016/j.psep.2022.04.034
23. Li Z, Gao P, Zhao X, Dong Z (2024) Potential and characteristics of rare-earth metals acid bioleaching from the rare-earth-rich tailings with the enriched functional bacterial consortium: Comparison between one-step and two-step processes. Chem Eng J 495:153492. https://doi.org/10.1016/j.cej.2024.153492
24. Gavrilescu M (2022) Microbial recovery of critical metals from secondary sources. Bioresour Technol 344:126208. https://doi.org/10.1016/j.biortech.2021.126208
25. Huang Y, Qiu Y, Zhang Z et al (2024) A perspective on molecular recognition technology for recovering critical metals from minerals and processing wastes. Sep Purif Technol 347:127734. https://doi.org/10.1016/j.seppur.2024.127734
26. Whitworth AJ, Vaughan J, Southam G et al (2022) Review on metal extraction technologies suitable for critical metal recovery from mining and processing wastes. Miner Eng 182:107537. https://doi.org/10.1016/j.mineng.2022.107537
27. Qing J, Zhao D, Zeng L et al (2024) Comprehensive recovery of rare earth elements and gypsum from phosphogypsum: a wastewater free process combining gravity separation and hydrometallurgy. J Rare Earths. https://doi.org/10.1016/j.jre.2024.01.013
28. Panda S, Costa RB, Shah SS et al (2021) Biotechnological trends and market impact on the recovery of rare earth elements from bauxite residue (red mud) – a review. Resour Conserv Recycl 171:105645. https://doi.org/10.1016/j.resconrec.2021.105645
29. Thomas BS, Bhattacharya S (2025) Quantification and recovery prospects of critical metals and rare earth elements in Victorian brown coal fly ash: a promising secondary source for critical metal extraction. Hydrometallurgy 232:106428. https://doi.org/10.1016/j.hydromet.2024.106428
30. Fu B, Hower JC, Zhang W et al (2022) A review of rare earth elements and yttrium in coal ash: Content, modes of occurrences, combustion behavior, and extraction methods. Prog Energy Combust Sci 88:100954. https://doi.org/10.1016/j.pecs.2021.100954
31. Sposato C, Catizzone E, Blasi A et al (2021) Towards the circular economy of rare earth elements: lanthanum leaching from spent FCC catalyst by acids. Processes. https://doi.org/10.3390/pr9081369
32. Ait Brahim J, Merroune A, Boulif R et al (2022) Efficient leaching process of rare earth, alkali and alkaline earth metals from phosphogypsum based on methanesulfonic acid (MSA) as green & eco-friendly lixiviant. RSC Adv 12:30639–30649. https://doi.org/10.1039/d2ra04124c
33. Chanouri H, Amal S, Mounir EM et al (2024) Beneficiation of rare earth elements contained in phosphogypsum using sequenced treatment process. J Environ Chem Eng 12:113148. https://doi.org/10.1016/j.jece.2024.113148
34. Dotto GL, Pinto D, Silva LFO et al (2024) Adsorption of rare earth elements (Ce3+, La3+, and Nd3+) and recovery from phosphogypsum leachate using a novel ZSM-5 zeolite. Colloids Surf A Physicochem Eng Asp 698:134549. https://doi.org/10.1016/j.colsurfa.2024.134549
35. Masmoudi-Soussi A, Hammas-Nasri I, Horchani-Naifer K, Férid M (2020) Rare earths recovery by fractional precipitation from a sulfuric leach liquor obtained after phosphogypsum processing. Hydrometallurgy 191:105253. https://doi.org/10.1016/j.hydromet.2020.105253
36. Gao Y, Hilbers M, Zhang H, Tanase S (2019) Designed synthesis of multiluminescent materials using lanthanide metal-organic frameworks and carbon dots as building-blocks. Eur J Inorg Chem. https://doi.org/10.1002/ejic.201900876
37. Ahn T, Kim JH, Yang H-M et al (2012) Formation pathways of magnetite nanoparticles by coprecipitation method. J Phys Chem C 116:6069–6076. https://doi.org/10.1021/jp211843g
38. Courtois J, Jin H, Chen H et al (2024) Superparamagnetic iron oxide nanoparticles functionalized with on-demand redox-responsive contractible coordination polymer brush as molecular actuator driven by π-dimerization. J Mol Liq 414:126303. https://doi.org/10.1016/j.molliq.2024.126303
39. Firouzi F, Sadrnezhaad SK (2024) Application of hydrophobic superparamagnetic nanoparticles in the solvent extraction of nickel aiming to accelerate phase disengagement. Colloids Surf A Physicochem Eng Asp 701:134927. https://doi.org/10.1016/j.colsurfa.2024.134927
40. Condomitti U, Almeida SN, Silveira AT Jr et al (2018) Green processing of strategic elements based on magnetic nanohydrometallurgy. J Braz Chem Soc. https://doi.org/10.21577/0103-5053.20180009
41. Menegatti de Melo F, Da AS, Santos A, Toma H (2017) Magnetophoresis of superparamagnetic nanoparticles applied to the extraction of lanthanide ions in the presence of magnetic field. NanoWorld J 3:38–43. https://doi.org/10.17756/nwj.2017-044
42. Lucas J, Lucas P, Le Mercier T et al (2015) Chapter 6 - Production of Rare Earth Metals and Alloys—Electrowinning. In: Lucas J, Lucas P, Le Mercier T et al (eds) Rare earths. Elsevier, Amsterdam, pp 93–108
43. Vinco JH, Botelho Junior AB, Duarte HA et al (2022) Purification of an iron contaminated vanadium solution through ion exchange resins. Miner Eng 176:107337. https://doi.org/10.1016/j.mineng.2021.107337

44. Sharifian S, Wang N-HL (2024) Resin-based approaches for selective extraction and purification of rare earth elements: a comprehensive review. J Environ Chem Eng 12:112402. https://doi.org/10.1016/j.jece.2024.112402
45. Quartarolli LF, Brandão BBNS, Silveira- Júnior AT et al (2022) Improving the lithium recovery using leached beta-spodumene residues processed by magnetic nanohydrometallurgy. Miner Eng 186:107747. https://doi.org/10.1016/j.mineng.2022.107747
46. Condomitti U, Zuin A, Silveira AT et al (2012) Magnetic nanohydrometallurgy: a promising nanotechnological approach for metal production and recovery using functionalized superparamagnetic nanoparticles. Hydrometallurgy 125(126):148
47. Leite S (2022) Using the SDGs for global citizenship education: definitions, challenges, and opportunities. Glob Soc Educ 20:401–413. https://doi.org/10.1080/14767724.2021.1882957
48. Opazo-Basáez M, Bustinza OF, Molina LM (2024) The effect of industrial solution services (ISS) on innovation performance: the moderating role of sustainable development goals (SDGs). J Clean Prod 455:142265. https://doi.org/10.1016/j.jclepro.2024.142265
49. Garcia-Saravia Ortiz-de-Montellano C, Samani P, van der Meer Y (2023) How can the circular economy support the advancement of the sustainable development goals (SDGs)? A comprehensive analysis. Sustain Prod Consum 40:352–362. https://doi.org/10.1016/j.spc.2023.07.003

Authors and Affiliations

Giovani Pavoski[1,2] · Denise Crocce Romano Espinosa[1] · Jorge Alberto Soares Tenório[1] · Wenying Liu[2]

✉ Giovani Pavoski
giovanipavoski@gmail.com

[1] LAREX – Laboratory of Recycling, Waste Treatment and Extraction, Chemical Engineering Department of Polytechnic School of University of São Paulo (USP), R. do Lago, 250 - Butantã, São Paulo, SP 05508-080, Brazil

[2] Department of Materials Engineering, The University of British Columbia (UBC), Frank Forward Building 309-6350 Stores Road, Vancouver, BC V6T 1Z4, Canada